Mlg1, a yeast acyltransferase located in ER membranes associated with mitochondria (MAMs), is involved in de novo synthesis and remodelling of phospholipids

Patricia Laquel, Sophie Ayciriex, François Doignon, Nadine Camougrand, Louise Fougère, Christophe Rocher, Valérie Wattelet-Boyer, Jean-jacques Bessoule, Eric Testet

Mlg1, a yeast acyltransferase located in ER membranes associated with mitochondria (MAMs), is involved in *de novo* synthesis and remodelling of phospholipids

Patricia Laquel [1 #], Sophie Ayciriex [2 #], François Doignon [1], Nadine Camougrand [3], Louise Fougère [1], Christophe Rocher [1], Valérie Wattelet-Boyer [1], Jean-Jacques Bessoule [1], Eric Testet [1, 4]

[1] Univ. Bordeaux, CNRS, LBM, UMR 5200, F-33140 Villenave d'Ornon, France.

[2] Univ Lyon, CNRS, Université Claude Bernard Lyon 1, ISA, UMR 5280, 5 rue de la Doua, F-69100 Villeurbanne, France.

[3] Univ. Bordeaux, CNRS, IBGC, UMR 5095, F-33000 Bordeaux, France.

[4] Bordeaux INP, LBM, UMR 5200, F-33140 Villenave d'Ornon, France

[#] Contributed equally

Address Correspondence to Dr Eric Testet . Univ. Bordeaux, CNRS, LBM, UMR 5200, F-33140 Villenave d'Ornon, France ; Email : eric.testet@ipb.fr

Running Title:

De novo synthesis and remodelling of phospholipids by *MLG1*

Abbreviations

AGC, automated gain control' AT, acyltransferase; PA, phosphatidic acid; PC, phosphatidylcholine; PE, phosphatidylethanolamine; PI, phosphatidylinositol; PS, phosphatidylserine; CL, cardiolipin; PG, phosphatidylglycerol; PIPs, phosphatidylinositol-phosphates; BSA, bovine serum albumin; CDP-DAG, cytidine diphosphate diacylglycerol; DAG, diacylglycerol; ER, endoplasmic reticulum; HPTLC, high-performance thin layer chromatography; IPTG, isopropyl ß-D-1-thiogalactopyranoside; MAMs, ER Membranes Associated with Mitochondria; MFQL, Molecular Fragmentation Query Language; MS, mass spectrometry; MTBE, methyl *tert*-butyl ether; ORF, open reading frame; 1-acyl lysoPL, 1-acyl-2-hydroxy-*sn*-glycero-3-phospholipid; 1-acyl lysoPA, 1-acyl-2-hydroxy-*sn*-glycero-3-phosphate; 2-acyl lysoPS, 2-acyl-1-hydroxy-*sn*-glycerol-3-phospho-L-serine; 2-acyl lysoPE, 2-acyl-1-hydroxy-*sn*-glycerol-3-phospho-L-ethanolamine; 1-acyl lysoPE, 1-acyl-2-hydroxy-*sn*-glycerol-3-phospho-L-ethanolamine; 1-acyl lysoPS, 1-acyl-2-hydroxy-*sn*-glycero-3-phospho-L-serine; 1-acyl lysoPC, 1-acyl-2-hydroxy-*sn*-glycerol-3-phosphocholine; 1-acyl lysoPG, 1-

acyl-2-hydroxy-*sn*-glycero-3-phospho-L-glycerol; 1-acyl lysoPI, 1-acyl-2-hydroxy-*sn*-glycero-3-phospho-L-inositol.

Key Words:

ER Mitochondria-associated membranes (MAMs), Lysolipid acyltransferase, Glycerophospholipid remodelling, *MLG1 :* hoMoLoG to *PSI1, Saccharomyces cerevisiae*

Conflicts of interest

The authors declare that they have no conflicts of interest.

Abstract

In cells, phospholipids contain acyl chains of variable lengths and saturation, features that affect their functions. Their *de novo* synthesis in the endoplasmic reticulum takes place *via* the cytidine diphosphate diacylglycerol (CDP-DAG) and Kennedy pathways, which are conserved in eukaryotes. PA is a key intermediate for all phospholipids (PI, PIPs, PS, PE, PC, PG and CL). The *de novo* synthesis of PA occurs by acylation of glycerophosphate leading to the synthesis of 1-acyl lysoPA and subsequent acylation of 1-acyl lysoPA at the *sn*-2 position. Using membranes from *Escherichia coli* overexpressing *MLG1*, we showed that the yeast gene *MLG1* encodes an acyltransferase leading specifically to the synthesis of PA from 1-acyl lysoPA. Moreover, after their *de novo* synthesis, phospholipids can be remodelled by acyl exchange with one and/or two acyl chains exchanged at the *sn*-1 or/and *sn*-2 position. Based on shotgun lipidomics of the reference and *mlg1*Δ strains, as well as biochemical assays for acyltransferase activities, we identified an additional remodelling activity for Mlg1p, namely incorporation of palmitic acid into the *sn*-1 position of PS and PE. By using confocal microscopy and subcellular fractionation, we also found that this acyltransferase is located in ER membranes associated with mitochondria, a finding that highlights the importance of these organelles in the global cellular metabolism of lipids.

Introduction

Eukaryotic cells are compartmentalised into organelles with distinct and characteristic phospholipid compositions that allow their proper biological function [1,2]. For each class of phospholipids, there are multiple molecular species defined by the nature of the acyl chains, which differ in terms of length, their degree of unsaturation and the position at *sn*-1 and *sn*-2 of the glycerol backbone. The composition of acyl chains differs according to the class of phospholipids. For example, in yeast PC and PE are enriched with unsaturated acyl chains while PI and PS have more saturated acyl chains [3]. In general, saturated acyl chains are esterified at the *sn*-1 position of the glycerol backbone while the *sn*-2 position is enriched in unsaturated acyl chains.

Most phospholipids are synthesised in the endoplasmic reticulum (ER) membranes and then be transported to other cellular compartments. In yeast, the *de novo* synthesis of phospholipids takes place *via* two biosynthetic pathways, the cytidine diphosphate diacylglycerol (CDP-DAG) and Kennedy pathways, which are largely conserved throughout the eukaryotic kingdoms. PA is synthesised from glycerol-3-phosphate or dihydroxyacetone-phosphate by two acylation steps and is a key intermediate for all phospholipids. PA can be converted to CDP-DAG, which serves as an intermediate for PI, PS, PG and CL. PS is decarboxylated to PE, which is then methylated to PC. PA can also be dephosphorylated to diacylglycerol (DAG), the precursor of PE and PC through the CDP-ethanolamine and CDP-choline pathways [4]. Both the biosynthetic pathways that lead to PC produce different sets of molecular species: the PE methylation route mainly produces di-unsaturated species, whereas the CDP-choline route produces a more diverse species profile [5]. Thus, all phospholipids are typically derived from PA. Nevertheless, following the action of phospholipase B, an acyltransferase (AT) acting on glycerophosphocholine (instead of glycero-3-phosphate) constitutes a third route to acylate the *sn*-1 position of the glycerol backbone [6].

In organelle membranes, neo-synthesised phospholipids acquire their specific acyl chain composition based on the molecular species–selectivity of enzymes involved in the biosynthetic routes. For example, Sct1p, one of the two ATs that catalyse the first step of the phospholipid synthesis, displays a preference towards 16-carbon fatty acids, while Gpt2p, the other AT that catalyses this reaction, can utilise a broad range of fatty acids as acyl donors [7]. Among the lysoPA AT activities identified, Slc1p, Ale1p and Loa1p have a selectivity for oleoyl-CoA, while Psi1p uses saturated substrates [8–10].

Following *de novo* synthesis, phospholipids can undergo remodelling in which one or both acyl chains are exchanged. The main classes of phospholipids are remodelled with rates depending on the class, the *sn*-1 or *sn*-2 position of the glycerol backbone and the

nature of supplied fatty acids [11]. Lands [12] was the first to describe the phospholipid exchange for PC. LysoPC formed by the action of a phospholipase A_2 can be re-acylated in a second step by an acyl-CoA:lysoPC AT. In this process known as the Lands cycle, the free fatty acid released from the *sn*-2 position of PC must be further activated to acyl-CoA [12] to enter lipid metabolism again.

In yeast, acyl chain exchange has been demonstrated by analysing the incorporation of radiolabelled fatty acid precursors. Using stable isotope labelling and mass spectrometry (MS), PC remodelling has been studied at the molecular species level [5,13,14]. A likely function of phospholipid chain remodelling in yeast is to adjust the lipid composition of membranes at the molecular species level to achieve the optimal membrane physical properties for a specific biological function. The characterisation of an AT in our group has established a link between the insertion of a specific molecular species of an acyl chain on a phospholipid and a biological function. The enrichment of stearic acid at the *sn*-1 position of PI, resulting from acyl chain remodelling by the *sn*-2 lysoPI AT encoded by *PSI1* [15], is required to maintain the quality of the cell polarity and secretory pathway [16,17]. In the present paper, we show that *MLG1,* a paralogue of *PSI1*, encodes a protein with AT activity involved in *de novo* PA biosynthesis as well as remodelling activity responsible for the palmitic acid enrichment of PS and PE. Moreover, by using confocal microscopy and subcellular fractionation, we demonstrate a particular localisation of this AT preferentially enriched in ER membranes associated with mitochondria (MAMs).

Results

Mlg1p displays *in vitro* acyl-CoA:lysoPA AT activity

The product of *MLG1 (hoMoLoG to PSI1),* alias *YDR018C*, belongs to the glycerolipid AT family. This protein has four regions containing the plsC domain. Motifs I (NHX_4D) and III (EGTR) represent the most conserved domains and are important for AT activity [18,19]. Figure 1 shows the conserved sequence of Mlg1p with the specific motifs of glycerolipid ATs from *Escherichia coli* (PlsC), *Saccharomyces cerevisiae* (Slc1p, Loa1p, Taz1p, Psi1p), *Caenorhabditis elegans* (ACL-8), *Mus musculus* (LYCAT) and *Homo sapiens* (AGPAT1) [8,15,20–24].

We tested whether Mlg1p has lysophospholipid AT activity. We cloned *MLG1* into pET-15b and expressed it in *E. coli* strain C41(DE3). After isopropyl ß-D-1-thiogalactopyranoside (IPTG) induction, we prepared *E. coli* membranes with or without recombinant Mlg1p, and analysed them for lysolipid AT activity using [^{14}C]oleoyl-CoA as an acyl donor and various unlabelled 1-acyl lysoPLs as acyl acceptors. Figure 2A shows that among the lyso-derivatives tested, only 1-acyl lysoPA was acylated by Mlg1p. We obtained

0.18 ± 0.06 nmol of phosphatidic acid synthesised per min and mg of membrane proteins when bacteria were transformed with the empty plasmid, corresponding to endogenous lysoPA AT activity [25], and 0.42 ± 0.11 nmol/min/mg when *MLG1* was overexpressed (Fig. 2B). These results indicate that the recombinant enzyme carried out acyl-CoA:lysoPA AT activity, which is specific for lysoPA. To confirm this result, we prepared microsomes from several strains: BY4742, *slc1*Δ, a strain that lacks the main lysoPA AT activity, and *slc1*Δ overexpressing constitutively *MLG1* and compared the rates of 1-acyl lysoPA acylation. The results shown in Fig. 2C confirm that Mlg1p could acylate 1-acyl lysoPA with oleoyl-CoA. To determine the substrate preference of Mlg1p towards acyl donors, we performed a substrate choice assay using [^{14}C]oleoyl-CoA in the presence of various unlabelled acyl-CoAs. The results in Fig. 2D show that as expected, the addition of unlabelled oleoyl-CoA decreased the label incorporation by 50%, whereas other acyl-CoAs did not decrease the incorporation of [^{14}C]oleoyl-CoA into PA to this extent. Hence, oleoyl-CoA is the preferred acyl donor.

The *slc1*Δ and *mlg1*Δ strains display similar lipid phenotypes

Next, we analysed and compared the lipid compositions of deletion mutants and the reference strain. Based on *in vitro* experiments suggesting that Mlg1p may have lysoPA AT activity, as a control in these assays we included a strain in which *SLC1* had been deleted. We grew cells on synthetic medium in the presence of dextrose or glycerol-ethanol, fermentable and respiratory carbon sources, respectively, from the early exponential phase with [^{14}C]acetate for about eight generations. In such a synthetic medium, in the absence of choline and ethanolamine precursors provided by the culture medium, the Kennedy pathway is restricted to recycling choline and ethanolamine derived from the degradation of PC and PE [26]. Hence, the CDP-DAG pathway is largely predominant and the major phospholipids are primarily synthesised from PA *via* CDP-DAG. We extracted total lipids and resolved them by using high-performance thin-layer chromatography (HPTLC) with a polar solvent system. The amount of radioactivity incorporated into total lipids was similar in the three strains (data not shown), which allows us to express the results as a percentage and to compare the lipidomes. The quantification of the incorporation in the neutral and polar lipids in both growth media (Fig. 3A and 3C) showed that *SLC1* deletion led to a significant decrease in polar lipid incorporation, compensated for by an increase in neutral lipids. There were similar results when comparing the lipidomes of the *mlg1*Δ and reference strains. The phospholipid class composition of the strain lacking Slc1p activity was strictly similar to that observed in the control, regardless of the growth medium used (Fig. 3B and 3D). This result indicates that a decrease in this lysoPA AT activity did not affect the overall phospholipid composition. Likewise, the phospholipid class composition of the *mlg1*Δ strain was similar to that of the reference strain.

Because we did not observe a difference in the phospholipid distribution in wild-type (WT) and mutant cells, we next performed pulse-labelling experiments to detect specific perturbations, to provide insight into the role of *MLG1* in the cell. Hence, we grew strains to the log phase and pulse labelled them with [^{14}C]oleic acid or [^{14}C]glycerol for 30 min. Focusing on the WT strain, it appears (Fig. 4A and 4B) that the major difference between the incorporation profiles of [^{14}C]oleic acid and [^{14}C]glycerol concern PC. For example, the incorporation of [^{14}C]oleic acid into PC and PS + PI was similar, whereas the incorporation of [^{14}C]glycerol was two times lower into PC than into PS + PI. Following a pulse with [^{14}C]glycerol, only lipids *de novo* synthesised were labelled, whereas using [^{14}C]oleic acid, in addition to *de novo* synthesised lipids, labelled oleoyl-CoA was incorporated into pre-existing unlabelled lipids. Our results highlight the fact that such remodelling mainly occurs in PC.

Compared with the reference strain, the *slc1*Δ strain showed a 35% decrease in PE incorporation and a 40% decrease in PS + PI incorporation; the *mlg1*Δ strain showed less pronounced decreases (Fig. 4A). The decrease in PC was only 13% in both mutants. We hypothesised that the relative weak decrease in the incorporation into PC is linked to additional incorporation of [^{14}C]oleoyl-CoA by remodelling (mainly) of PC. Under these conditions, following a pulse using [^{14}C]glycerol, for which the incorporation only takes place by *de novo* synthesis, the decrease in incorporation into PC should be similar to that observed for PE and PS + PI. The results supported this hypothesis: consistent with the decrease in the incorporation into PS + PI following a pulse with oleic acid or with glycerol, there was a 40% decrease in the incorporation of [^{14}C]glycerol into PC for the *slc1*Δ strain (Fig. 4B). When we compared the effect of oleic acid or glycerol pulses for the *mlg1*Δ and reference strains, we observed a similar lipid phenotype as for *slc1*Δ. Such a result strengthens the fact that Mlg1p and Slc1p display the same enzymatic activity**.** Overall, these results, obtained with both *in vitro* and *in vivo* approaches, are consistent with the idea that *MLG1* encodes a protein with lysoPA AT activity.

Deletion of *MLG1* alters the fatty acid composition of PS and PE

The above lipid analyses revealed similar profiles of phospholipid classes *in vivo* but did not provide information on their fatty acid composition. Hence, we performed a shotgun lipidomics experiment to compare the lipidome of the *mlg1*Δ strain with the reference strain to investigate specific defects at the molecular species level. Shotgun lipidomics revealed that the percentage of palmitic acid–containing PS and PE molecular species was significantly reduced in the *mlg1*Δ strain: PS 16:0_16:1, PS 16:0_18:1, PE 16:0_16:1 and PE 16:0_18:1. This decrease was mainly compensated for by an increase in the 16:1/16:1 and 16:1_18:1 molecular species (Fig. 5). We observed an inverse phenotype in PS and PE molecular

species when we profiled the strain overexpressing *MLG1*. These results observed in the *mlg1*Δ and *MLG1*-overexpressing strains suggest a specific acyl chain exchange in PS and PE. Several studies have shown, either by MS [8,10,27,28] or a biochemical approach using phospholipase A_2 [11,15], that saturated fatty acids are mainly located at the *sn*-1 position in phospholipids. Moreover, when cells are cultured in the presence of radiolabelled palmitic acid, there is a selective incorporation of label into the *sn*-1 position of PS [11]. Thus, our lipidomics results suggest that Mlg1p is an AT that specifically enriches palmitic acid at the *sn*-1 position of the glycerol backbone of PS and PE. Nevertheless, at this stage of the study, we cannot rule out the possibility that the phenotype observed for PE is linked to the fact that PE is derived directly from PS but retains the same defect in acyl chains, and thus only PS would be remodelled by Mlg1p.

By comparing the observed phenotype for PS and PE in the *mlg1*Δ strain, we observed a strictly inverse lipid phenotype in the lysoPA, PA, PC and DAG classes (Fig. 5 and 6): *mlg1*Δ cells produced significantly higher levels of molecular species with a palmitic acyl chain, whereas there was lower level in cells overexpressing *MLG1*. Because the acyl chain donor used by Mlg1p to transfer palmitic acid to the *sn*-1 position of lysoPS would be palmitoyl-CoA, we hypothesised that because the remodelling activity of Mlg1p is absent in the deletion mutant, palmitoyl-CoA is redirected towards the ATs that acylate glycerol-3-phosphate during *de novo* synthesis. PA is the direct precursor of DAG and, consistently, the latter has the same fatty acid composition as PA (Fig. 5 and 6). There were no significant changes for the PI molecular species (Fig. 5), which could be explained by the high specificity of Psi1p that directs stearic acid at the *sn*-1 position of this lipid. To confirm the nature of the acyl acceptor and to verify that Mlg1p uses palmitoyl-CoA as an acyl donor, we correlated the lipidomic results with a biochemical approach using AT activity assays.

Mlg1p directs palmitic acid to the *sn*-1 position of PS and PE

To evaluate the 2-acyl lysoPS activity of Mlg1p, we performed an AT activity assay by using [^{14}C]palmitoyl-CoA as an acyl donor and 2-acyl lysoPS as an acyl acceptor in the presence of homogenates obtained from several strains: WT, *mlg1*Δ and WT overexpressing *MLG1*. Due to the lack of commercially available 2-acyl lysoPS, we prepared an extemporaneous preparation of this lysolipid using PS hydrolysed by the *Rhizopus orizae* lipase. As a control to check the specificity of the AT, we included enzymatic assays with [^{14}C]oleic-CoA and commercially available 1-18:1 lysoPS. We did not detect PS synthesis in assays without added lysoPS (Fig. 7A). In contrast, due to the activity of the AT Ale1p that specifically incorporates unsaturated acyl-CoAs [9,14,29–31] into PS, we noted a strong incorporation of labelled oleoyl-CoA at the *sn*-2 position of 1-18:1 lysoPS regardless of the source of the homogenate – that is, with or without *MLG1*. Using homogenates from the WT or *mlg1*Δ

strain, this activity was almost undetectable in the presence of palmitoyl-CoA (Fig. 7A). The weak PS synthesis observed in the presence of palmitoyl-CoA when *MLG1* was overexpressed (Fig. 7A, upper part) could be explained by the presence of 2-18:1 lysoPS, a potential substrate of Mlg1p that could have contaminated the commercial 1-18:1 lysoPS product. Indeed, according to the supplier, 1-18:1 lysoPS may contain up to 10% of this isomer. However, we cannot exclude the possibility that overproduced Mlg1p catalysed a slight acylation of 1-18:1 lysoPS.

When we performed experiments in the presence of a preparation of 2-acyl lysoPS and labelled palmitoyl-CoA, we observed prominent synthesis of labelled PS when the homogenate was obtained from a strain overexpressing the *MLG1* gene, whereas there was no synthesis with homogenates from the WT or *mlg1*Δ strain (Fig. 7A, lower part). These results indicate that overexpressed Mlg1p can acylate 2-acyl lysoPS with palmitoyl-CoA and that this enzyme is not abundant enough to detect its activity in a homogenate obtained from the reference strain. These results also indicate that Ale1p activity does not synthesise PS in the presence of palmitoyl-CoA and 2-acyl lysoPS. In other words, using the substrates 2-acyl lysoPS and palmitoyl-CoA, we strictly quantified the Mlg1p activity. In the presence of oleoyl-CoA, we measured trace PS synthesis with homogenates (Fig. 7A, lower part). This residual activity, observed independently of the presence or absence of the *MLG1* gene, indicates on the one hand that 2-acyl lysoPS is not a substrate of Ale1p and, on the other hand, that 2-acyl lysoPS is not significantly converted to its 1-acyl lysoPS isomer during preparation or assay procedures (otherwise, Ale1p-catalysed PS synthesis would be observed in the presence of oleoyl-CoA).

Next, we investigated whether 2-acyl lysoPE is a substrate for Mlg1p. For this endeavour, we measured incorporation of [^{14}C]palmitoyl-CoA in the presence of an extemporaneous preparation of 2-acyl lysoPE. PE synthesis doubled when using a homogenate prepared from a WT strain overexpressing the *MLG1* gene instead of a homogenate from the *mlg1*Δ strain (Fig. 7B). This result indicates that Mlg1p also possesses the ability to acylate 2-acyl lysoPE *in vitro*. Because palmitoyl-CoA is not a substrate of Ale1p (see above), the significant level of PE synthesis in the absence of the *MLG1* gene suggests that the yeast possesses a second gene encoding an enzyme with acyl-CoA:2-acyl lysoPE AT activity, although it has not yet been characterised.

To sum up, our enzymatic assays indicate that (1) Mlg1p can acylate 2-acyl lysoPS and 2-acyl lysoPE, (2) this activity is selective for palmitoyl-CoA and (3) in *S. cerevisiae*, the sole Mlg1p has 2-acyl lysoPS palmitoyltransferase activity. These results confirm the hypothesis we formulated during the lipidomics experiment. Hence, both the *in vivo* and *in vitro* approaches indicate that *MLG1* encodes an enzyme that also has palmitoyl-CoA:2-acyl lysoPS and palmitoyl-CoA:2-acyl lysoPE AT activities. Note that Psi1p possesses both acyl-

CoA:lysoPA AT activity and remodelling activity at the *sn*-1 position of lysoPI with a saturated fatty acid [10,15] and other ATs possess several distinct activities [10,24]. Therefore, it appears that Mlg1p has a second AT activity in addition to its acyl-CoA:lysoPA AT activity.

Mlg1p is localised in MAMs

We analysed the subcellular distribution of Mlg1p by using confocal microscopy and subcellular fractionation. As a first control, we checked that the wild-type strain BY4741 without any external fluorochrome showed no emission with a maximum intensity at 512 nm (corresponding to the GFP spectrum), but only a very weak cytosolic background signal in a few cells with a maximum intensity of emission at 550 nm (likely due to yeast flavin autofluorescence [32]). Then we observed that the cells only labelled with green or red fluorochrome at the *MLG1* or *ILV3* genes show a similar pattern of fluorescence as a tubular mitochondrial network (Fig. 8). Afterwards reference strain BY4741 carrying Mlg1p and Ilv3p (a mitochondrial protein [33]), tagged at their locus with 3xGFP and tdimer2(12), respectively, showed a co-localised fluorescent signal for most of the observed cells (87%), suggesting a mitochondrial distribution for Mlg1p (Fig.9A and 9B).

In addition, more convincing than the merge to demonstrate a co-localisation are the values of the co-localisation parameters (tM1 and tM2), as well as the two-dimensional (2D) histograms of pixel distribution (scatterplots). The values of tM1 and tM2 above the auto-threshold channel 2 (red) and 1 (green) were 0.66 ± 0.15 and 0.88 ± 0.07 (n = 71), respectively, and therefore are compatible with a predominant localisation of Mlg1p in the mitochondrial network. In addition, the scatterplots (Fig. 9A) indicate complete co-localisation of Mlg1p1 and Ilv3p, with a pixel distribution along a straight line and a slope that depends on the fluorescence ratio between the two channels [34]. Z-stack images allowed a maximum intensity projection (using the Zen-black software) showing the juxtaposition in space of the green and red signals, and a 3D image created by using the IMARIS software which reported the surfaces of the objects observed (Fig. 9C). A strong concordance appeared between the surface of the mitochondrial membranes drawn by the red signal (Ilv3p marker) and the green signal (Mlg1p). In different places the green signal came out and suggested a location of Mlg1p in membranes associated with – and closed to - mitochondria, which could be the ER membranes, *i.e.* the MAMs.

We also implemented another combination with Pho88p (an ER landmark [33]) tagged with the red fluorochrome tdimer2(12); only a few cells showed co-localisation with Mlg1p (13%) (Fig. 9A and 9B). The resulting low values of the tM1 and tM2 coefficients (0.06 ± 0.06 and 0.04 ± 0.05, respectively; n = 50) also indicate weak co-localisation of Mlg1p with the ER compartment. In addition, the scatterplots obtained for Mlg1p and Pho88p evidenced

a pixel distribution spread all around the regression line. Nevertheless, we did not observe exclusive staining with pixel intensities distributed along the axes, which would be the sign of a total exclusion and absence of co-localisation [34]. Thus, whereas there was a complete co-localisation with Ilv3p, the scatterplot for Mlg1p compared with the Pho88p landmark revealed a partial co-localisation for these proteins. These results suggest that Mlg1p is associated with an ER fraction attached to mitochondria, namely MAMs. This has been evidenced for other enzymes involved in phospholipid metabolism, such as Ale1p [9].

To confirm the Mlg1p sub-cellular location, we obtained fractions from crude mitochondria by centrifugation onto a 20%–60% continuous sucrose gradient. We first characterised fractions by western blotting using anti-Por1 and anti-Dpm1 antibodies, specific landmark for the outer mitochondrial membranes and the ER membranes, respectively (Fig 10A). As expected, Por1p was highly detected in the densest fractions and barely quantifiable in the two lightest fractions, indicating that the latter were largely devoid of mitochondria (Fig.10B). Conversely, the Dpm1 marker was predominantly detected in these lightest fractions. The membranes found in these fractions therefore corresponded to ER membranes that remained associated with mitochondria after successive centrifugations and washings, but removed from mitochondria after centrifugation onto the sucrose gradient. This corresponds to the definition of MAMs [35]. In agreement, the specific activity of Ale1p, a biochemical marker of MAMs [9] was 2-3-fold higher in fraction 2 than in fraction 10 (Fig. 11A). The (slight) Ale1p activity detected within fraction 10 might suggest that a proportion of MAMs remained bound to the mitochondrial outer membrane, even after the centrifugation on the 20%–60% continuous sucrose gradient.

We also used fractions 2 and 10 as a protein source to measure the specific 2-acyl-lyso-PS activity of Mlg1p (in control, we performed assays as a function of time and the 2-acyl lysoPS amount, as well as controls without 2-acyl lysoPS or using MAMs from the *mlg1Δ* strain, data not shown). Fraction 2 was the most highly enriched in Mlg1p activity, displaying (similarly to Ale1p) a 2–3-fold higher specific activity than fraction 10 (Figure 11B). This clearly indicated that Mlg1p has the same cellular localization as Ale1p. These results obtained by using a biochemical approach alongside the fluorescence microscopy findings (showing that Mlg1p is located in ER membranes associated with mitochondria) indicated that Mlg1p is preferentially located in MAMs, a sub-fraction of the ER tightly bound to the mitochondrial membranes. As noted for Ale1p, the (slight) Mlg1p activity detected within fraction 10 might suggest that a proportion of MAMs remained bound to the mitochondrial outer membrane, even after the centrifugation on the sucrose gradient. Nevertheless, Mlg1p localization and activity has been found at the ER-mitochondria interface, but that to rule out a specific localization at MAM vs mitochondria will deserve further investigation in future studies (i.e. by doing ER-mito-Mlg1p triple

stainings, super-resolution microscopy, immuno-electron microscopy, subcellular isolation of MAM and mitochondria and validation by using proper ER, MAM and mitochondria markers …).

Discussion

Using inverse genetics approaches, researchers have identified several putative lysolipid ATs belonging to the glycerolipid AT family in yeast. The common feature of these enzymes is the similarity to the *E. coli* PlsC sequence, characterised by the presence of four conserved domains [19]. The first AT of this family characterised in yeast was Slc1p, which has been described as the major lysoPA AT [36]. *In vitro* AT assays indicated that Slc1p is able to incorporate [^{14}C]acyl-CoA into various lysolipids, with lysoPA being the preferential acceptor [24]. Subsequently, our group has characterised three other lysolipid ATs: (1) Taz1p, the yeast paralogue of tafazzin, is involved in cardiolipin remodelling [22] and displays lysoPC AT activity [22]; (2) Psi1p is responsible for the specific stearic acid enrichment of the *sn*-1 position of neo-synthesised PI [10,15] and also mediates the acyl-CoA-dependent acylation of lysoPA [10]; and (3) Loa1p is a redundant lysoPA AT that is associated with lipid particles and involved in triacylglycerol homeostasis [8]. Besides Slc1p, Loa1p and Psi1p, other enzymes not belonging to the glycerolipid AT family but showing lysoPA AT activity have been identified in yeast: Ale1p, a member of the membrane-bound *O*-AT family, is a lysolipid AT with broad specificity for acyl acceptor, including lysoPA [9,24,29–31,37], and Ict1p is a soluble enzyme with lysoPA AT activity [38]. Tgl3p, Tgl4p and Tgl5p, which are lipases associated with lipid droplets, are also able to acylate lysoPA *in vitro* [39,40].

In the present study, we focused on *MLG1*, a paralogue of *PSI1*. It is very likely that following an ancestral whole duplication of the genome [41–43], the *MLG1* and *PSI1* genes are present (with about 10 genes) in a conserved chromosomal environment and positioned on chromosomes IV and II, respectively [44]. In agreement, in *Candida albicans*, a pre-whole genome duplication yeast [45], only one protein, encoded from the C6_01300W locus, shows strong similarities to Mlg1p and Psi1p. During evolution, changes in the genes may have slightly modified the function of the associated proteins. In our case, *MLG1* and *PSI1* both encode ATs, but we have demonstrated that even through the substrate specificities (lysophospholipid and acyl chain) are different, both of these enzymes are involved in phospholipid remodelling with saturated fatty acids. Because effective maintenance of membrane properties is essential for survival in a variable and complex environment, lipid acyl chain remodelling is an essential mechanism from bacteria to eukaryotic cells when adapting to changing environmental conditions [46–49]. Moreover, in mammals, for example

the synthesis and degradation of some bioactive lipids and their precursors involves ATs that catalyse lipid remodelling with fatty acids such as arachidonic acid, the precursor of prostaglandins and leukotrienes [50]. In the present study, moderate differences in the lipid compositions between the *MLG1* deletion mutant and the wild type strain were shown, but this did not lead to a strong phenotype (growth rate, cell viability, etc.) of the mutant. Nevertheless, we previously studied the *psi1*Δ mutant for which PI as well as its phosphoinositide derivatives are depleted of stearic acyl chain acids associated with the *sn*-1 position, and we showed that phosphoinositide species containing stearic acid (and synthesised *via* remodelling) control cell polarity and the secretory pathway *via* the Cdc42p module [16,17]. Similarly, Mlg1p enhances the amount of saturated fatty acids associated with the *sn*-1 position of PS and could also be involved in the control of cell polarity, because PS has a determining role for the activity and clusters formation of the Cdc42 protein (the master regulator of cell polarity). More precisely, Cdc42 modulation of PS (and cooperatively with phosphoinositides) occurs *via* the Cdc24–Bem1 complex [51]. Perhaps in concert with the presence of saturated (stearic) acid at the *sn*-1 position of phosphoinositides, the presence of saturated (palmitic) acid at the *sn*-1 position of PS modulates the targeting of the Cdc42 regulators Bem1 and Cdc24, and therefore controls cell polarity.

Materials and methods

Materials

HPTLC silica gel 60 F 254 20×10 cm plates were obtained from Merck (Darmstadt, Germany). [^{14}C]acetic acid, [^{14}C]oleoyl-CoA, [^{14}C]palmitoyl-CoA, [^{14}C]oleic acid and [^{14}C]glycerol were obtained from Perkin Elmer Life Sciences (Boston, MA, USA). 1-18:1 lysoPS was purchased from Avanti Polar Lipids (Birmingham, USA). Other lysophospholipids, phospholipids and *R. oryzae* lipase were procured from Sigma-Aldrich (St. Louis, MO, USA).

Yeast strains and media

The *S. cerevisiae* strains used in this study are listed in Table 1. Standard techniques for culturing the yeast were used and the composition of rich fermentescible (YPD) or non-fermentescible medium (YPGE) and synthetic complete (SC) (2% dextrose), SC-GE (3% glycerol, 2% ethanol) or SC-Gal (2% galactose) medium for yeast cultures have been reported elsewhere [52]. Yeast strains were grown at 30°C.

Plasmid constructs

For production of Mlg1p in *E. coli* C41(DE3), a fragment corresponding to the *MLG1* open

reading frame (ORF) was cloned into pET15-15b (Novagen, Darmstadt, Germany)). *MLG1* overexpression in the *slc1*Δ strain was implemented after cloning the *MLG1* ORF into the pVT102-U-GW plasmid, which places the coding sequences under the control of the strong *ADH1* constitutive promoter [53,54]. For *MLG1* overexpression, a *Bam*HI-*Not*I fragment corresponding to the *MLG1* ORF was inserted under the control of the tetO promoter in pCM189 [55]. For the localisation of Mlg1p *in vivo*, we generated a construct tagged at the C terminus with green fluorescent protein, using the integrative yeast vector pRS305-3xGFP (generously provided by Dr Isabelle Sagot and Dr David Pellman), which contains three tandem copies of the GFP gene. We inserted the last 1188 bp (*MLG1*) before the stop codon into pRS305-3xGFP and targeted integration to the *MLG1* locus after digestion by *Hin*dIII.

Yeast strain constructs

Mlg1p and Psi1p were tagged at their C-terminal end with 3xGFP at their chromosomal loci using pRS305-3xGFP. Strains used for co-localisation analyses were also tagged with the red fluorochrome tdimer2(12) fused in frame at the 3′ end of *ILV3* [33] or to *PHO88* ORFs (a generous gift from Dr I. Sagot, Bordeaux). The BY4741 Erg6-mRFP1 strain was obtained from Invitrogen (Carlsbad, USA) [56].

Preparation of *E. coli* homogenates and membranes

The *E. coli* strains used in this work are listed in Table 1. Cloning, ectopic expression of the *MLG1* gene in *E. coli* and isolation of *E. coli* membranes were carried out according to Testet *et al.* [22]. To prepare cell homogenates, 5 x 10^7 cells were broken with glass beads in a buffer containing 0.6 M mannitol, 2 mM EGTA, 10 mM Tris maleate (pH 6.8) plus protease inhibitor cocktail (Roche). Lysates were centrifuged at 800 *g* for 10 min and the supernatants were used for enzymatic dosages.

1-acyl lysoPA AT assays

AT activities associated with membranes of *E. coli* expressing *MLG1* were measured according to Ayciriex *et al.* [8]. In microsomal membranes from the BY4742, *slc1*Δ or *slc1*Δ overexpressing *MLG1* strains, 1-acyl lysoPA AT activity was evaluated in 100 µl of assay mixture (25 mM Tris-HCl, pH 7) containing 1 nmol of 1-acyl lysoPA and 1 nmol of [^{14}C]oleoyl-CoA. The reactions were incubated at 30°C and then stopped by the addition of 200 µl of 0.7% perchloric acid and 1 ml of chloroform/methanol (2:1, v/v). After centrifugation, the organic phase was isolated, and the aqueous phase was re-extracted with 1 ml of chloroform. The combined lipid extracts were dried and re-dissolved in 100 µl of chloroform/methanol (2:1, v/v), and 20 µl of lipid extract was purified by TLC, using 20 × 10 cm HPTLC plates. Lipids were separated using the solvent system

chloroform/methanol/H_2O/25% NH_4OH (30:17:2:1, v/v/v/v) [57]. Lipid identity was based on the mobility of known standards, and the amount of labelled lipids was analysed by phosphorimaging.

2-acyl lysoPS and 2-acyl lysoPE AT assays

The 2-acyl lysoPLs are especially unstable; neutral or alkaline conditions accelerate the partial isomerisation of 2-acyl lysoPL to 1-acyl lysoPL. To determine whether Mlg1p is a 2-acyl lysoPS AT, it was necessary to synthesise a substrate not contaminated by its isomer. It has been shown that intramolecular acyl isomerisation does not occur under acidic conditions [58]. Hence, 2-acyl lysoPS was synthesised by hydrolysing PS with phospholipase A_1 using an acidic buffer. 2-Acyl lysoPS was prepared as described previously [15], with slight modifications. A chloroform/methanol organic phase containing approximately 120 nmol of bovine brain PS was evaporated in a gas chromatography vial. Four hundred microliters of diethyl ether and 400 µl of 50 mM Tris maleate (pH 5.8) and 10 mM $CaCl_2$ containing 160 units of *R. oryzae* lipase were added and mixture was incubated for 15 min at room temperature with vigorous stirring. After incubation, the diethyl ether phase was evaporated, the aqueous phase was transferred to a microcentrifuge tube and the reaction product was extracted with 400 µl of 1-butanol. Twenty microliters of the resulting 1-butanol phase were taken and evaporated to dryness in a glass tube for an enzymatic assay. Based on comparison with the TLC migration pattern of a known amount of commercial 1-18:1 lysoPS strained with the ninhydrin reagent, the amount of 2-acyl lysoPS contained in 20 µl was estimated as 1 nmol.

If isomerisation occurs during the reaction with the *R. orizae* lipase at an acidic pH or during the acyltransferase assay at a neutral pH, then the 1-acyl lysoPS isomer (a substrate of Ale1p) would have been formed. Therefore, the purity of the product was checked by carrying out an AT assay with the freshly prepared product in the presence of [^{14}C]oleoyl-CoA (the preferential substrate of Ale1p as an acyl donor) and a homogenate as enzyme source. Under these conditions, there was no PS synthesis. Such a result highlighted the absence of 1-acyl lysoPS in the freshly prepared product, and therefore the purity of the synthesised 2-acyl lysoPS. The 2-acyl lysoPE preparation was prepared according the same protocol.

In cell homogenates from the BY4742, *mlg1*Δ or BY4742 overexpressing *MLG1* strains, lysolipid AT reactions were conducted in 100 µl of assay mixture (50 mM Tris-HCl [pH 7.2] and 2 mM EGTA) containing 1 nmol of [^{14}C]oleoyl-CoA or [^{14}C]palmitoyl-CoA; 10 µg of homogenate; and 1 nmol of 2-acyl lysoPS preparation, 2-acyl lysoPE preparation or commercial 1-18:1 lysoPS. The reaction was incubated at 30°C for 10 min. 2-Acyl lysoPS AT activities associated with microsomal membranes and crude mitochondria were determined

using 0.5 nmol of [^{14}C]palmitoyl-CoA, 1 nmol of 2-acyl lysoPS preparation and 1–2.5 µg proteins for 5 min. 2-Acyl lysoPS AT activities associated with mitochondria and MAMs purified by centrifugation on a sucrose gradient were determined using 0.5 nmol of [^{14}C]palmitoyl-CoA, 1 nmol of 2-acyl lysoPS preparation and 5 µg of protein for 15 min. 1-LysoPS AT activity (*i.e.* Ale1p activity) was determined with 0.5 nmol of [^{14}C]oleoyl-CoA, 1 nmol of commercial 1-18:1 lysoPS and 0.1–0.4 µg of protein for 5 min. The labelled lipids were analysed as described above. The protein concentration was determined using BCA protein assay kit (Sigma-Aldrich), with bovine serum albumin (BSA) as the standard.

Metabolic labelling

For steady-state labelling, 25 ml samples of *mlg1*Δ, *slc1*Δ or BY4742 cells, grown at 30°C in SC or SC-GE medium to an OD_{600} of 0.01, were labelled with [^{14}C]acetic acid (10 µCi/assay) over approximately eight generations [59]. For pulse labelling with oleic acid, cells grown at 30°C in YPGE medium to the exponential phase (OD_{600} = 0.1) were labelled with 2 µCi of [^{14}C]palmitic acid or [^{14}C]oleic acid for 15 min. For pulse labelling with glycerol, cells grown in YPGE medium were washed four times with phosphate-buffered saline and once with SC medium maintained at 30°C before adding 2 µCi of [^{14}C]glycerol for 30 min. Then cells were pelleted by centrifugation, and the supernatant was removed. To extract lipids from whole cells, 200 µl of 0.7% perchloric acid and 1 ml of chloroform/methanol (2:1, v/v) were added, and cell suspensions were vigorously shaken with glass beads (three times for 30 s with a TissueLyser II). The lipids were extracted and analysed as described above.

Lipid extraction for shotgun lipidomics

Lipid extraction was adapted from Fu *et al*. [60]. Yeast cell pellets were homogenised in 300 µl of cold isopropanol with zirconia beads (Ø 0.5 mm) for 10 min at 30 Hz and 4°C (two cycles) with a TissueLyser II. The protein concentration of the homogenates was determined with the BCA protein assay. Next, ~50 µg of total protein was extracted according to a modified version of the methyl *tert*-butyl ether (MTBE) lipid extraction procedure [61]. Briefly, 700 µl of MTBE/methanol (10:3, v/v) containing one synthetic internal standard representative for each lipid class was added to the dried homogenates. Samples were vortexed at 4°C for 1h. Phase separation was produced by adding 140 µl of water and agitating for 15 min at 4°C, followed by centrifugation (13,400 rpm for 15 min at 4°C). The upper organic phase was collected, dried down and reconstituted in 600 µl of chloroform/methanol (1:2, v/v). Finally, 10 µl of total lipid extract was diluted with 90 µl of isopropanol/methanol/chloroform (4:2:1, v/v/v) containing 7.5 mM ammonium formate for high-resolution MS.

Shotgun lipidomics

Shotgun lipidomics analyses were performed on a Q Exactive instrument (Thermo Fischer Scientific, Bremen, Germany) equipped with a TriVersa NanoMate robotic nanoflow ion source (Advion BioSciences, Ithaca, NY, USA) using nanoelectrospray chips with a diameter of 4.1 µm. The ion source was controlled by the Chipsoft 8.3.1 software (Advion BioSciences). The ionisation voltage was +0.96 kV in the positive ion mode and -0.96 kV in the negative ion mode. The backpressure was set at 1.25 psi in both modes by polarity switching according to a previous study [62]. The temperature of the ion transfer capillary was set to 200°C and the S-lens RF level was 50%. Fourier-transform mass spectra were acquired within the range of *m/z* 400–1000 from 0 to 1.5 min in the positive ion mode and then within the range of *m/z* 350–1000 from 4.2 to 5.7 min in the negative mode at a mass resolution of 140,000 (at *m/z* 200), with an automated gain control (AGC) of 3×10^6 and a maximal injection time of 3000 ms. For FT MS/MS (the PRM method), the micro scans were set to 1; the isolation window was set to 1 Da; the stepped normalised collision energy was 15, 25 and 35; AGC was 2×10^4; and the maximum injection time was 650 ms. All acquired data was filtered by PeakStrainer that can be found at gitlab (https://git.mpi-cbg.de/labShevchenko/PeakStrainer/wikis/About) [63]. Lipids were identified by using the LipidXplorer 1.2.7 software [64]. Molecular Fragmentation Query Language (MFQL) queries were compiled for the neutral lipid (DAG), phospholipid (PC, PE, PI, PS and PA) and lysophospholipid (1-acyl lysoPA and 1-acyl lysoPC) classes. Identification of the lipid class relied on accurately determining the intact lipid masses (mass accuracy > 5 ppm). The identification of the lipid molecular species relied on inspection of the tandem mass spectra in both polarities of the polar head group fragments and fatty acid moieties. Lipids were quantified by comparing the isotopically corrected abundances of their molecular ions with the abundances of internal standards of the same lipid class. The abundance of lipid species is presented as mol%.

Lipid annotation

In this study, the yeast lipid molecules were identified at the molecular species level according to the shorthand notation provided by LIPID MAPS and the International lipidomics society [65,66]. Fragmentation (MS/MS) of lipid species delivers subspecies information in terms of fatty acyl chain composition. Hence, phospholipid species were annotated accordingly to the exact acyl moieties composition and their *sn* position when known [27,28]. For example, PS 16:0_16:1 indicates phosphatidylserine with palmitic acid (16:0) and palmitoleic acid (16:1), for which the exact position (*sn*-1 or *sn*-2) esterified to the glycerol backbone cannot be discriminated (denoted by '_' between the fatty acyl chains). Conversely, PS 16:0/16:1 indicates phosphatidylserine, in which the fatty acyl chain moiety

16:0 is located at the *sn*-1 position of the glycerol backbone and the fatty acyl chain moiety 16:1 is located at the *sn*-2 position of the glycerol backbone. The slash ('/') symbol separates the fatty acyl chains, meaning that the *sn*-position on the glycerol backbone can be resolved. The PL 18:0_16:1 molecular species are either undetectable or present in low concentrations in yeast cells [27,28]. Hence, for simplicity the isobaric combinations 16:0_18:1 or 18:0_16:1 have been reduced to their main molecular species.

Fluorescence microscopy

The samples were prepared as described in a previous paper [17]. To avoid bleed through, the images were acquired sequentially for the red and green channels using narrow band emission filters. GFP fluorescence was observed at 500–600 nm, with the maximum intensities of the emission spectra at 510 and 530 nm, after excitation of the live cells with a laser at 488 nm. In the case of double-labelling cells with GFP and a red fluorochrome, fluorescence was observed using the Airyscan super-resolution mode on the LSM880 microscope (Zeiss, Oberkochen, Germany) at, respectively, 510 nm with band pass filters of 420–480 and 495–550 nm (following excitation at 488 nm) and 600 nm with a band pass filter of 570–620 nm and a long-pass filter of 645 nm (following excitation at 561 nm). Single controls were used to assess bleed-through. Live cell confocal imaging for Z-stacks acquisitions were carried out using the scan mode and the superresolution Airyscan mode of Airyscan1 module of a Zeiss LSM 880 using 63X oil-immersion objective (NA 1.4) with a Z-step of 210 nm through 4.64 µm thickness (22 slices).

Mander's tM1 and tM2 co-localisation coefficient measurements

Using the FIJI software from ImageJ, and particularly Coloc 2 from the co-localisation plugins, the Manders co-localisation coefficients tM1 and tM2 were calculated after background subtraction and using auto-threshold to avoid including pixels below the image's threshold in the analysis according to the Costes method [67]. The co-localisation threshold plugins generate scatterplots and correlation coefficients. For the tM1 and tM2 coefficients, only the pixels where both channel 1 and channel 2 are above their respective threshold (*i.e.* the upper right quadrant of the scatterplot) are considered with the regression line plotted along with the threshold level for the green channel 1 (vertical line) and the red channel 2 (horizontal line). The data shown are the mean ± standard error of co-localisation between Mlg1p and the Ilv3p mitochondrial landmark (n = 71 cells) and between Mlg1p and the Pho88p ER landmark (n = 42 cells).

3D Modelling

Z-stack images of cells labelled with 3xGFP-tagged Mlg1p and Ilv3p fused to tdimer2(12) were processed using the airyscan processing software and the maximum intensity projection method. The 3D surface reconstruction mode of the Zen black 2.3 SP1 software (basic, advanced and full resolution) create an image from the airyscan processed image. Using the Bitplane Imaris10 software a 3D image which reports the surfaces of the objects observed (called Surface rendering) was created. Prior to do the surface rendering, thanks to the Imaris software, a median filter were applied on the airyscan processed image file (5x5 for channel red and 3x3x3 for channel green).

Mitochondrial purification and density gradient centrifugation analysis

The method used in this study has been described in previous publications [68,69]. Cells were harvested and washed three times with water and incubated at 28°C for 15 min in a pre-incubating buffer (0.5 M β-mercaptoethanol and 0.1 M Tris, pH 9.3). After three washes with Tris KCl buffer (10 mM Tris and 0.5 M KCl, pH 7), cells were digested in digestion buffer (1.35 M sorbitol, 10 mM citric acid, 30 mM Na_2HPO_4, 1 mM EGTA and zymolyase 20T at 20 mg/g dry weight). Spheroplasts were washed twice in isotonic buffer (0.75 M sorbitol, 0.4 M mannitol, 10 mM Tris maleate and 0.1% BSA, pH 6.8) and resuspended in homogenisation buffer (0.6 M mannitol, 10 mM Tris maleate, 2 mM EGTA and 0.2% BSA, pH 6.8). Spheroplasts were broken using a blender. Unbroken spheroplasts and heavy cell compartments were pelleted by centrifugation at 700 *g* for 10 min, and the supernatant was centrifuged at 12,000 *g* for 10 min. The pellet was resuspended in the final buffer (0.6 M mannitol, 2 mM EGTA and 10 mM Tris maleate, pH 6.8) and then centrifuged at 700 g for 10 min. The supernatant was removed and centrifuged at 12,000 *g* for 10 min to pellet crude mitochondria. After an additional centrifugation step of 30,000 *g* for 1 h, mitochondria were washed three times and then resuspended in the final buffer with protease inhibitors. One milligram of protein was loaded on a 20%–60% continuous sucrose gradient and centrifuged overnight at 134,000 *g*. Fractions were then collected from the top to the bottom and analysed by western blotting with the anti-Porin antibody (Invitrogen).

Author Contributions

P.L., S.A., F.D., L.F., C.R., N.C.,V.W.B. designed and performed the experiments; P.L., S.A., F.D., L.F., C.R., N.C.,V.W.B. and J.J.B. analyzed the data; and J.J.B., F.D., P.L., E.T. wrote the manuscript.

Acknowledgements

Imaging were done on the Pôle Imagerie du Végétal, appended to the Bordeaux Imaging Centre (http://www.bic.u-bordeaux.fr/) which is a part of the France BioImaging Infrastructure

(https://france-bioimaging.org/) (ANR-11-INBS-004), with technical support provided by Dr Brigitte Batailler, Lysiane Brocard and Dr Clément Chambaud. TLC analyses were performed at Bordeaux Metabolome Facility-MetaboHUB (ANR-11-INBS-0010). Targeted experiments for phospholipid analysis were conducted at the Institute of Analytical Sciences (UMR5280 CNRS UCBL).

Data availability statement

The data that support the findings of this study are available from the corresponding author (eric.testet@ipb.fr) upon reasonable request.

References

1 Zinser E, Sperka-Gottlieb CD, Fasch EV, Kohlwein SD, Paltauf F & Daum G (1991) Phospholipid synthesis and lipid composition of subcellular membranes in the unicellular eukaryote Saccharomyces cerevisiae. *J Bacteriol* **173**, 2026–2034.

2 Zachowski A (1993) Phospholipids in animal eukaryotic membranes: transverse asymmetry and movement. *Biochem J* **294 (Pt 1)**, 1–14.

3 Schneiter R, Brugger B, Sandhoff R, Zellnig G, Leber A, Lampl M, Athenstaedt K, Hrastnik C, Eder S, Daum G, Paltauf F, Wieland FT & Kohlwein SD (1999) Electrospray ionization tandem mass spectrometry (ESI-MS/MS) analysis of the lipid molecular species composition of yeast subcellular membranes reveals acyl chain-based sorting/remodeling of distinct molecular species en route to the plasma membrane. *J Cell Biol* **146**, 741–54.

4 McMaster CR & Bell RM (1994) Phosphatidylcholine biosynthesis in Saccharomyces cerevisiae. Regulatory insights from studies employing null and chimeric sn-1,2-diacylglycerol choline- and ethanolaminephosphotransferases. *J Biol Chem* **269**, 28010–28016.

5 Boumann HA & de Kroon AIPM (2005) The contributions of biosynthesis and acyl chain remodelling to the molecular species profile of phosphatidylcholine in yeast. *Biochem Soc Trans* **33**, 1146–1149.

6 Głąb B, Beganovic M, Anaokar S, Hao M-S, Rasmusson AG, Patton-Vogt J, Banaś A, Stymne S & Lager I (2016) Cloning of Glycerophosphocholine Acyltransferase (GPCAT) from Fungi and Plants: A NOVEL ENZYME IN PHOSPHATIDYLCHOLINE SYNTHESIS. *J Biol Chem* **291**, 25066–25076.

7 Zheng Z & Zou J (2001) The initial step of the glycerolipid pathway: identification of glycerol 3-phosphate/dihydroxyacetone phosphate dual substrate acyltransferases in Saccharomyces cerevisiae. *J Biol Chem* **276**, 41710–41716.

8 Ayciriex S, Le Guédard M, Camougrand N, Velours G, Schoene M, Leone S, Wattelet-Boyer V, Dupuy J-W, Shevchenko A, Schmitter J-M, Lessire R, Bessoule J-J & Testet E (2012) YPR139c/LOA1 encodes a

novel lysophosphatidic acid acyltransferase associated with lipid droplets and involved in TAG homeostasis. *Mol Biol Cell* **23**, 233–246.

9 Riekhof WR, Wu J, Jones JL & Voelker DR (2007) Identification and characterization of the major lysophosphatidylethanolamine acyltransferase in Saccharomyces cerevisiae. *J Biol Chem* **282**, 28344–28352.

10 Shui G, Guan XL, Gopalakrishnan P, Xue Y, Goh JS, Yang H & Wenk MR (2010) Characterization of substrate preference for Slc1p and Cst26p in Saccharomyces cerevisiae using lipidomic approaches and an LPAAT activity assay. *PLoS One* **5**, e11956.

11 Wagner S & Paltauf F (1994) Generation of glycerophospholipid molecular species in the yeast Saccharomyces cerevisiae. Fatty acid pattern of phospholipid classes and selective acyl turnover at sn-1 and sn-2 positions. *Yeast* **10**, 1429–37.

12 Lands WE (1960) Metabolism of glycerolipids. 2. The enzymatic acylation of lysolecithin. *J Biol Chem* **235**, 2233–2237.

13 De Smet CH, Cox R, Brouwers JF & de Kroon AIPM (2013) Yeast cells accumulate excess endogenous palmitate in phosphatidylcholine by acyl chain remodeling involving the phospholipase B Plb1p. *Biochim Biophys Acta* **1831**, 1167–1176.

14 Tanaka K, Fukuda R, Ono Y, Eguchi H, Nagasawa S, Nakatani Y, Watanabe H, Nakanishi H, Taguchi R & Ohta A (2008) Incorporation and remodeling of extracellular phosphatidylcholine with short acyl residues in Saccharomyces cerevisiae. *Biochim Biophys Acta* **1781**, 391–399.

15 Le Guédard M, Bessoule JJ, Boyer V, Ayciriex S, Velours G, Kulik W, Ejsing CS, Shevchenko A, Coulon D, Lessire R & Testet E (2009) PSI1 is responsible for the stearic acid enrichment that is characteristic of phosphatidylinositol in yeast. *FEBS J* **276**, 6412–24.

16 Doignon F, Laquel P, Testet E, Tuphile K, Fouillen L & Bessoule JJ (2016) Requirement of phosphoinositides containing stearic acid to control cell polarity. *Mol Cell Biol* **36**, 765–780.

17 Laquel P, Testet E, Tuphile K, Cullin C, Fouillen L, Bessoule J-J & Doignon F (2022) Phosphoinositides containing stearic acid are required for interaction between Rho GTPases and the exocyst to control the late steps of polarized exocytosis. *Traffic* **23**, 120–136.

18 Heath RJ & Rock CO (1998) A conserved histidine is essential for glycerolipid acyltransferase catalysis. *J Bacteriol* **180**, 1425–1430.

19 Lewin TM, Wang P & Coleman RA (1999) Analysis of amino acid motifs diagnostic for the sn-glycerol-3-phosphate acyltransferase reaction. *Biochemistry* **38**, 5764–71.

20 Imae R, Inoue T, Nakasaki Y, Uchida Y, Ohba Y, Kono N, Nakanishi H, Sasaki T, Mitani S & Arai H (2012) LYCAT, a homologue of C. elegans acl-8, acl-9, and acl-10, determines the fatty acid composition of phosphatidylinositol in mice. *J Lipid Res* **53**, 335–47.

21 Imae R, Inoue T, Kimura M, Kanamori T, Tomioka NH, Kage-Nakadai E, Mitani S & Arai H (2010) Intracellular phospholipase A1 and acyltransferase, which are involved in Caenorhabditis elegans stem cell divisions, determine the sn-1 fatty acyl chain of phosphatidylinositol. *Mol Biol Cell* **21**, 3114–24.

22 Testet E, Laroche-Traineau J, Noubhani A, Coulon D, Bunoust O, Camougrand N, Manon S, Lessire R & Bessoule J-J (2005) Ypr140wp, “the yeast tafazzin”, displays a mitochondrial

lysophosphatidylcholine (lyso-PC) acyltransferase activity related to triacylglycerol and mitochondrial lipid synthesis. *Biochem J* **387**, 617–626.

23 Agarwal AK, Sukumaran S, Cortés VA, Tunison K, Mizrachi D, Sankella S, Gerard RD, Horton JD & Garg A (2011) Human 1-acylglycerol-3-phosphate O-acyltransferase isoforms 1 and 2: biochemical characterization and inability to rescue hepatic steatosis in Agpat2(-/-) gene lipodystrophic mice. *J Biol Chem* **286**, 37676–37691.

24 Benghezal M, Roubaty C, Veepuri V, Knudsen J & Conzelmann A (2007) SLC1 and SLC4 encode partially redundant acyl-coenzyme A 1-acylglycerol-3-phosphate O-acyltransferases of budding yeast. *J Biol Chem* **282**, 30845–30855.

25 Coleman J (1990) Characterization of Escherichia coli cells deficient in 1-acyl-sn-glycerol-3-phosphate acyltransferase activity. *J Biol Chem* **265**, 17215–17221.

26 Horvath SE, Wagner A, Steyrer E & Daum G (2011) Metabolic link between phosphatidylethanolamine and triacylglycerol metabolism in the yeast Saccharomyces cerevisiae. *Biochimica et Biophysica Acta (BBA) - Molecular and Cell Biology of Lipids* **1811**, 1030–1037.

27 Buré C, Ayciriex S, Testet E & Schmitter JM (2012) A single run LC-MS/MS method for phospholipidomics. *Anal Bioanal Chem* **405**, 203–13.

28 Ejsing CS, Sampaio JL, Surendranath V, Duchoslav E, Ekroos K, Klemm RW, Simons K & Shevchenko A (2009) Global analysis of the yeast lipidome by quantitative shotgun mass spectrometry. *Proc Natl Acad Sci U S A* **106**, 2136–41.

29 Riekhof WR, Wu J, Gijón MA, Zarini S, Murphy RC & Voelker DR (2007) Lysophosphatidylcholine metabolism in Saccharomyces cerevisiae: the role of P-type ATPases in transport and a broad specificity acyltransferase in acylation. *J Biol Chem* **282**, 36853–36861.

30 Chen Q, Kazachkov M, Zheng Z & Zou J (2007) The yeast acylglycerol acyltransferase LCA1 is a key component of Lands cycle for phosphatidylcholine turnover. *FEBS Lett* **581**, 5511–5516.

31 Jain S, Stanford N, Bhagwat N, Seiler B, Costanzo M, Boone C & Oelkers P (2007) Identification of a novel lysophospholipid acyltransferase in Saccharomyces cerevisiae. *J Biol Chem* **282**, 30562–30569.

32 Monici M (2005) Cell and tissue autofluorescence research and diagnostic applications. *Biotechnol Annu Rev* **11**, 227–256.

33 Jimenez L, Laporte D, Duvezin-Caubet S, Courtout F & Sagot I (2014) Mitochondrial ATP synthases cluster as discrete domains that reorganize with the cellular demand for oxidative phosphorylation. *J Cell Sci* **127**, 719–26.

34 Bolte S & Cordelières FP (2006) A guided tour into subcellular colocalization analysis in light microscopy. *J Microsc* **224**, 213–232.

35 Vance JE (1990) Phospholipid synthesis in a membrane fraction associated with mitochondria. *J Biol Chem* **265**, 7248–7256.

36 Nagiec MM, Wells GB, Lester RL & Dickson RC (1993) A suppressor gene that enables Saccharomyces cerevisiae to grow without making sphingolipids encodes a protein that resembles an Escherichia coli fatty acyltransferase. *J Biol Chem* **268**, 22156–22163.

37 Tamaki H, Shimada A, Ito Y, Ohya M, Takase J, Miyashita M, Miyagawa H, Nozaki H, Nakayama R & Kumagai H (2007) LPT1 encodes a membrane-bound O-acyltransferase involved in the acylation of lysophospholipids in the yeast Saccharomyces cerevisiae. *J Biol Chem* **282**, 34288–34298.

38 Ghosh AK, Ramakrishnan G & Rajasekharan R (2008) YLR099C (ICT1) encodes a soluble Acyl-CoA-dependent lysophosphatidic acid acyltransferase responsible for enhanced phospholipid synthesis on organic solvent stress in Saccharomyces cerevisiae. *J Biol Chem* **283**, 9768–9775.

39 Rajakumari S & Daum G (2010) Janus-faced enzymes yeast Tgl3p and Tgl5p catalyze lipase and acyltransferase reactions. *Mol Biol Cell* **21**, 501–510.

40 Rajakumari S & Daum G (2010) Multiple functions as lipase, steryl ester hydrolase, phospholipase, and acyltransferase of Tgl4p from the yeast Saccharomyces cerevisiae. *J Biol Chem* **285**, 15769–15776.

41 Dujon B (2006) Yeasts illustrate the molecular mechanisms of eukaryotic genome evolution. *Trends Genet* **22**, 375–387.

42 Koszul R, Caburet S, Dujon B & Fischer G (2004) Eucaryotic genome evolution through the spontaneous duplication of large chromosomal segments. *EMBO J* **23**, 234–243.

43 Kellis M, Birren BW & Lander ES (2004) Proof and evolutionary analysis of ancient genome duplication in the yeast Saccharomyces cerevisiae. *Nature* **428**, 617–624.

44 Wolfe KH & Shields DC (1997) Molecular evidence for an ancient duplication of the entire yeast genome. *Nature* **387**, 708–713.

45 Rozpędowska E, Galafassi S, Johansson L, Hagman A, Piškur J & Compagno C (2011) Candida albicans--a pre-whole genome duplication yeast--is predominantly aerobic and a poor ethanol producer. *FEMS Yeast Res* **11**, 285–291.

46 Liu X, Ma D, Zhang Z, Wang S, Du S, Deng X & Yin L (2019) Plant lipid remodeling in response to abiotic stresses. *Environmental and Experimental Botany* **165**, 174–184.

47 Röttig A & Steinbüchel A (2013) Acyltransferases in Bacteria. *Microbiol Mol Biol Rev* **77**, 277–321.

48 Yu L, Zhou C, Fan J, Shanklin J & Xu C (2021) Mechanisms and functions of membrane lipid remodeling in plants. *The Plant Journal* **107**, 37–53.

49 Renne MF, Bao X, De Smet CH & de Kroon AIPM (2015) Lipid Acyl Chain Remodeling in Yeast. *Lipid Insights* **8**, 33–40.

50 Yamashita A, Hayashi Y, Nemoto-Sasaki Y, Ito M, Oka S, Tanikawa T, Waku K & Sugiura T (2014) Acyltransferases and transacylases that determine the fatty acid composition of glycerolipids and the metabolism of bioactive lipid mediators in mammalian cells and model organisms. *Prog Lipid Res* **53**, 18–81.

51 Meca J, Massoni-Laporte A, Martinez D, Sartorel E, Loquet A, Habenstein B & McCusker D (2018) Avidity-driven polarity establishment via multivalent lipid-GTPase module interactions. *EMBO J* **38**.

52 Rose MD, Winston F & Hieter P (1990) *Methods in Yeast Genetics: A Laboratory Course Manual* Cold Spring Harbor Laboratory Press, Cold Spring Harbor, New York.

53 Domergue F, Vishwanath SJ, Joubes J, Ono J, Lee JA, Bourdon M, Alhattab R, Lowe C, Pascal S, Lessire R & Rowland O (2010) Three Arabidopsis fatty acyl-coenzyme A reductases, FAR1, FAR4, and

FAR5, generate primary fatty alcohols associated with suberin deposition. *Plant Physiol* **153**, 1539–54.

54 Monfort A, Finger S, Sanz P & Prieto JA (1999) Evaluation of different promoters for the efficient production of heterologous proteins in baker's yeast. *Biotechnology Letters* **21**, 225–229.

55 Gari E, Piedrafita L, Aldea M & Herrero E (1997) A set of vectors with a tetracycline-regulatable promoter system for modulated gene expression in Saccharomyces cerevisiae. *Yeast* **13**, 837–48.

56 Huh WK, Falvo JV, Gerke LC, Carroll AS, Howson RW, Weissman JS & O'Shea EK (2003) Global analysis of protein localization in budding yeast. *Nature* **425**, 686–91.

57 Handloser D, Widmer V & Reich E (2008) Separation of Phospholipids by HPTLC – An Investigation of Important Parameters. *Journal of Liquid Chromatography & Related Technologies* **31**, 1857–1870.

58 Okudaira M, Inoue A, Shuto A, Nakanaga K, Kano K, Makide K, Saigusa D, Tomioka Y & Aoki J (2014) Separation and quantification of 2-acyl-1-lysophospholipids and 1-acyl-2-lysophospholipids in biological samples by LC-MS/MS. *J Lipid Res* **55**, 2178–2192.

59 Gaspar ML, Aregullin MA, Jesch SA & Henry SA (2006) Inositol induces a profound alteration in the pattern and rate of synthesis and turnover of membrane lipids in Saccharomyces cerevisiae. *J Biol Chem* **281**, 22773–85.

60 Fu T, Knittelfelder O, Geffard O, Clément Y, Testet E, Elie N, Touboul D, Abbaci K, Shevchenko A, Lemoine J, Chaumot A, Salvador A, Degli-Esposti D & Ayciriex S (2021) Shotgun lipidomics and mass spectrometry imaging unveil diversity and dynamics in Gammarus fossarum lipid composition. *iScience* **24**, 102115.

61 Matyash V, Liebisch G, Kurzchalia TV, Shevchenko A & Schwudke D (2008) Lipid extraction by methyl-tert-butyl ether for high-throughput lipidomics. *J Lipid Res* **49**, 1137–1146.

62 Schuhmann K, Almeida R, Baumert M, Herzog R, Bornstein SR & Shevchenko A (2012) Shotgun lipidomics on a LTQ Orbitrap mass spectrometer by successive switching between acquisition polarity modes. *J Mass Spectrom* **47**, 96–104.

63 Schuhmann K, Thomas H, Ackerman JM, Nagornov KO, Tsybin YO & Shevchenko A (2017) Intensity-Independent Noise Filtering in FT MS and FT MS/MS Spectra for Shotgun Lipidomics. *Anal Chem* **89**, 7046–7052.

64 Herzog R, Schuhmann K, Schwudke D, Sampaio JL, Bornstein SR, Schroeder M & Shevchenko A (2012) LipidXplorer: a software for consensual cross-platform lipidomics. *PLoS One* **7**, e29851.

65 Liebisch G, Vizcaíno JA, Köfeler H, Trötzmüller M, Griffiths WJ, Schmitz G, Spener F & Wakelam MJO (2013) Shorthand notation for lipid structures derived from mass spectrometry. *J Lipid Res* **54**, 1523–1530.

66 O'Donnell VB, Dennis EA, Wakelam MJO & Subramaniam S (2019) LIPID MAPS: Serving the next generation of lipid researchers with tools, resources, data, and training. *Sci Signal* **12**, eaaw2964.

67 Costes SV, Daelemans D, Cho EH, Dobbin Z, Pavlakis G & Lockett S (2004) Automatic and quantitative measurement of protein-protein colocalization in live cells. *Biophys J* **86**, 3993–4003.

68 Légiot A, Céré C, Dupoiron T, Kaabouni M, Camougrand N & Manon S (2019) Mitochondria-Associated Membranes (MAMs) are involved in Bax mitochondrial localization and cytochrome c release. *Microb Cell* **6**, 257–266.

69 Glick BS & Pon LA (1995) [14] Isolation of highly purified mitochondria from Saccharomyces cerevisiae. In *Methods in Enzymology* pp. 213–223. Academic Press.

70 Miroux B & Walker JE (1996) Over-production of proteins in Escherichia coli: mutant hosts that allow synthesis of some membrane proteins and globular proteins at high levels. *J Mol Biol* **260**, 289–98.

71 Corpet F (1988) Multiple sequence alignment with hierarchical clustering. *Nucleic Acids Res* **16**, 10881–10890.

Table 1. *Saccharomyces cerevisiae* and *Escherichia coli* strains used in this study

Strain	Genotype	Source
BY4742	*MATα, his3Δ1, leu2Δ0, lys2Δ0, ura3Δ0*	Euroscarf
BY4741	*MAT***a,** *his3Δ1, leu2Δ0, met15Δ0, ura3Δ0*	Euroscarf
*mlg1*Δ	BY4742, *mlg1::KanMX4*	Euroscarf
*ale1*Δ	BY4742, *ale1::KanMX4*	Euroscarf
*slc1*Δ	BY4742, *slc1::KanMX4*	Euroscarf
*psi1*Δ	BY4742, *psi1::KanMX4*	Euroscarf
BY4742 pCM189	BY4742, pCM189 *(URA3)*	This work
*mlg1*Δ pCM189	*mlg1::KanMX4* pCM189 *(URA3)*	This work
BY4742 pCM189-*MLG1*	BY4742, pCM189-*MLG1 (URA3)*	This work
BY4742 pVT102-U-GW	BY4742, pVT102-U-GW *(URA3)*	This work
*slc1*Δ pVT102-U-GW	*slc1*Δ, pVT102-U-GW *(URA3)*	This work
*slc1*Δ pVT102-U-GW-*MLG1*	*slc1*Δ, pVT102-U-GW-*MLG1 (URA3)*	This work
BY4741 Mlg1-3xGFP	*MLG1::3xGFP (LEU2*	This work
BY4741 Mlg1-3xGFP Ilv3-tdimer2(12)	*MLG1::3xGFP (LEU2); ILV3::tdimer2(12)(URA3)*	This work
BY4741 Mlg1-3xGFP Pho88-tdimer2(12)	*MLG1::3xGFP (LEU2); PHO88::tdimer2(12)(URA3)*	This work
E. coli C41(DE3)	*F-ompT gal hsdSB (rB-mB-) dcm lonλDE3 pLysS*	[70]
E. coli C41(DE3) pET15-15b	C41(DE3), pET15-15b (Amp^R)	This work
E. coli C41(DE3) pET15-15b-*MLG1*	C41(DE3), pET15-15b-*MLG1* (Amp^R)	This work

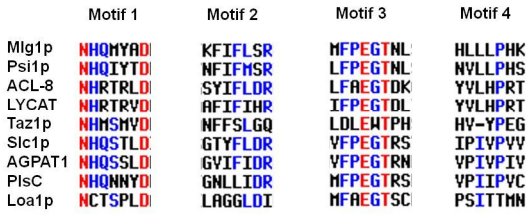

Fig. 1. Analysis of conserved amino acids of glycerolipid AT motifs in *Saccharomyces cerevisiae* (Mlg1p, Psi1p, Slc1p, Loa1p and Taz1p), *Escherichia coli* (PlsC), *Caenorhabditis elegans* (ACL-8), *Mus musculus* (LYCAT) and *Homo sapiens* (AGPAT1).

Multiple alignments of conserved motifs were extracted from protein multi-alignments realised using the MultAlin program [71]. High consensus colour: red; Low consensus colour: blue; Neutral colour: black.

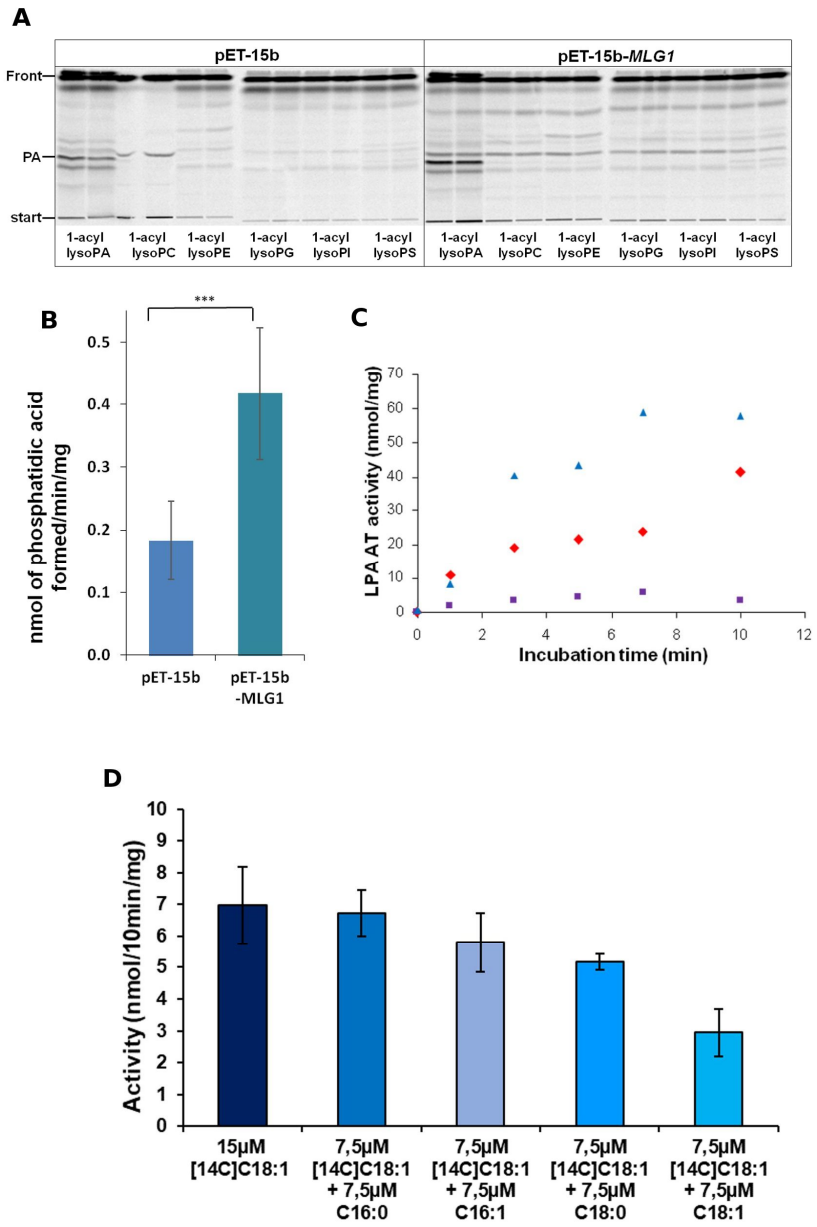

Fig. 2. Acyl-CoA:1-acyl lysoPA AT activity associated with membranes of *Escherichia coli* producing Mlg1p or with microsomes of *Saccharomyces cerevisiae*.

(A and B) Membrane proteins (5 µg) of *E. coli* C41(DE3) transformed with pET-15b or with pET-15b containing the coding sequence of *MLG1* were incubated with 0.5 nmol [^{14}C]oleoyl-CoA and 1 nmol of various 1-acyl lysoPL. After incubation for 5 min at 30°C, lipids were extracted and analysed as described in the Material and methods. (A) TLC obtained with lipids extracted from membrane proteins *E. coli* C41(DE3) transformed with pET-15b or with pET-15b containing the *MLG1* coding sequence. (B) Graphical representation of phosphatidic acid formed with membrane proteins of C41(DE3) *E. coli* pET-15b and membrane proteins of *E. coli* C41(DE3) pET-15b containing the coding sequence of *MLG1*. The results are presented as the mean ± standard deviation of six independent biological replicates from two distinct membrane preparations. Statistical analysis was done with an unpaired, two-tailed *t*-test: ***p < 0.001. (C) LysoPA AT activities were determined by incubating for different times 10 µg of microsomes purified from the BY4742 (diamond), *slc1*Δ (square) and *slc1*Δ + *MLG1* (triangle) strains with 2 nmol LPA and 1 nmol of [^{14}C]oleoyl-CoA. (D) LysoPA AT activities were determined by incubating for 10 min 10 µg of microsomes purified from the BY4742 strain with 2 nmol of 1-acyl lysoPA and 15 µM of [^{14}C]oleoyl-CoA or 7.5 µM of [^{14}C]oleoyl-CoA and 7.5 µM of each unlabelled acyl-CoA. The results are presented as the mean ± standard deviation for three determinations.

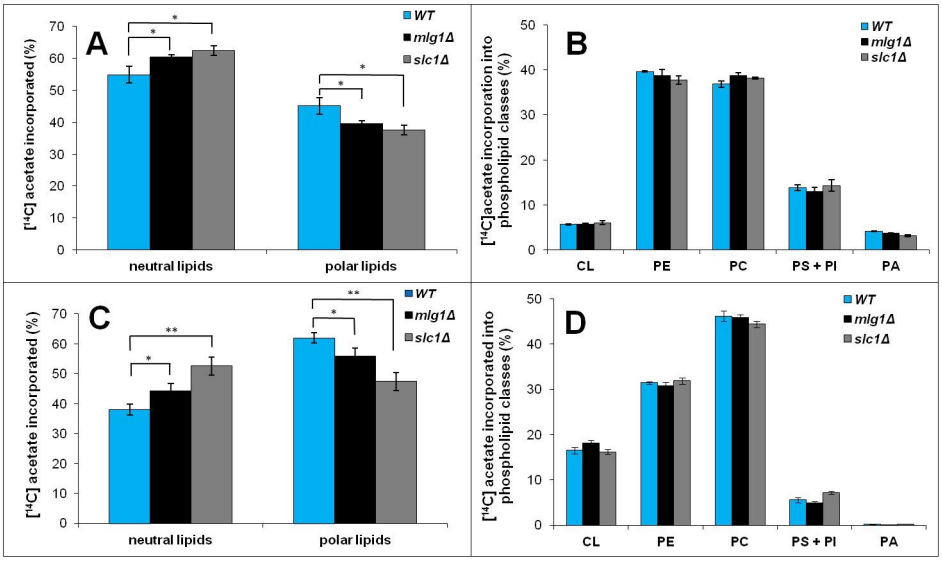

Fig. 3. The *slc1*Δ and *mlg1*Δ strains display similar lipid phenotypes.

Cells were grown to an OD_{600} of 0.01 on synthetic defined media in the presence of dextrose (SC) (A and B) or glycerol-ethanol (SC-GE) (C and D) and labelled to steady state with [^{14}C]acetate during eight generations. Lipids were extracted and separated by TLC as described in the Materials and methods. (A and C) Label incorporated into neutral and polar

lipids. (B and D) Incorporation into the phospholipid classes. Light grey bar: WT strain; grey bar: *mlg1*Δ strain; dark grey bar: *slc1*Δ strain. The results are presented as the mean ± standard deviation from one experiment performed in triplicate and are representative of two distinct experiments. Statistical analysis was done with an unpaired, two-tailed *t*-test: **p* < 0.05; ***p* < 0.01.

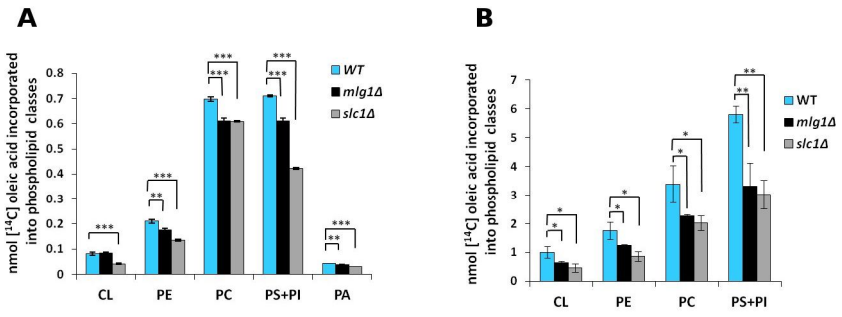

Fig. 4. Incorporation of [^{14}C]oleic acid and [^{14}C]glycerol into phospholipids.

Cells grown until the early logarithmic phase (OD_{600} = 0.1) in YPGE medium were labelled for 30 min. Lipids were extracted and separated by TLC as described in the Materials and methods. Incorporation of [^{14}C]oleic acid (A) or [^{14}C]glycerol (B) into the major phospholipids. Light grey bar: WT strain; grey bar: *mlg1*Δ strain; dark grey bar: *slc1*Δ strain. The results are presented as the mean ± standard deviation from one experiment performed in triplicate and are representative of two distinct experiments. Statistical analysis was done with an unpaired, two-tailed *t*-test: **p* < 0.05; ***p* < 0.01; ****p* < 0.001.

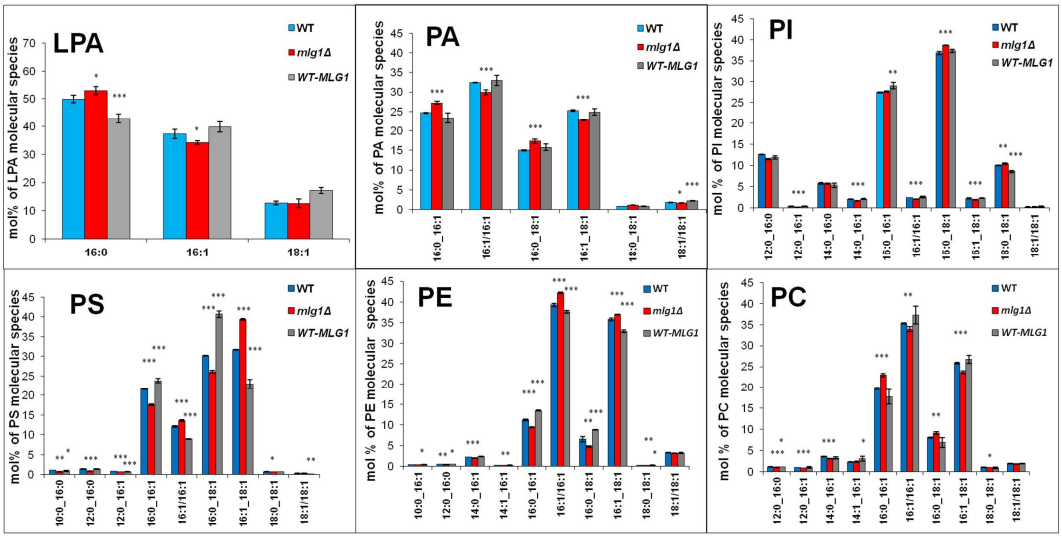

Fig. 5. Lipid profiling of the WT, *mlg1*Δ and WT overexpressing *MLG1* strains.

Cells were grown on synthetic defined media in the presence of 2% dextrose (SC) and harvested at the logarithmic phase. Lipids were extracted from yeast cells according to the Materials and methods. Lipid species were profiled in the Fourier-transform MS negative mode on a QExactive mass spectrometer and lipid classes were identified and quantified by the LipidXplorer software. Lipid molecular species were determined by fragmentation experiments. The abundance of lipid species is presented as mol%. The results are presented as the mean ± standard deviation (n = 4 independent analyses). Statistical analysis was done with an unpaired, two-tailed *t*-test: *$p < 0.05$; **$p < 0.01$; ***$p < 0.001$).

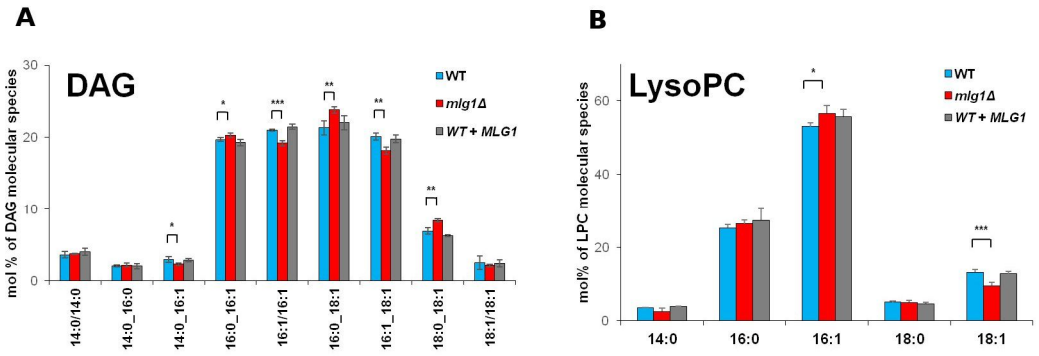

Fig. 6. DAG and lysoPC profiling of the WT, *mlg1*Δ and WT overexpressing constitutively *MLG1* strains.

(A) DAG. (B) LysoPC. Cells were grown on synthetic defined media in the presence of 2% dextrose (SC) and harvested at the logarithmic phase. Lipids were extracted from yeast cells according to a previous study [60]. Lipid species were profiled in the Fourier-transform MS negative mode on a QExactive mass spectrometer and lipid classes were identified and quantified by the LipidXplorer software [64]. Lipid molecular species were determined by fragmentation experiments. The abundance of lipid species is presented as mol%. The data are presented as the mean ± standard deviation (n = 4 independent analyses). Statistical analysis was done with an unpaired, two-tailed *t*-test was used: *$p < 0.05$; **$p < 0.01$; ***$p < 0.001$.

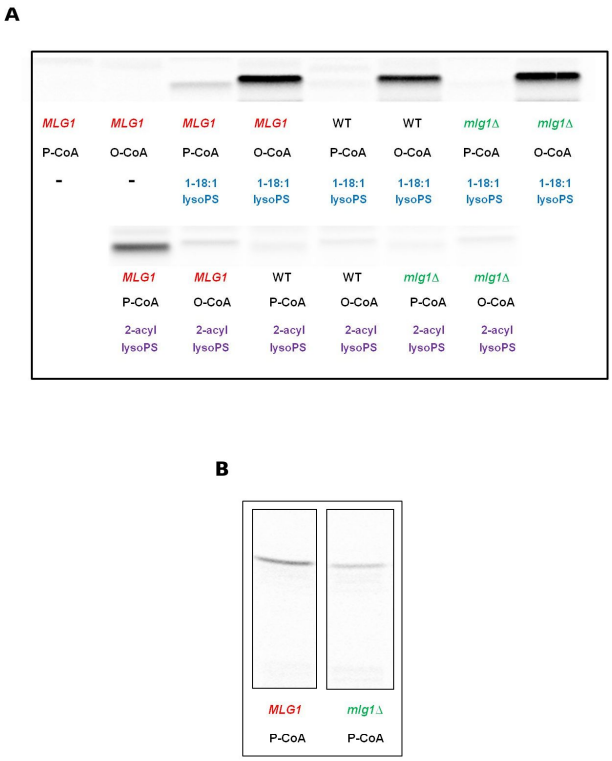

Fig. 7. Homogenate from the WT strain overexpressing *MLG1* displays palmitoyl-CoA:2-acyl lysoPS and palmitoyl-CoA:2-acyl lysoPE AT activities.

Protein homogenates (10 µg) were prepared from the WT, *mlg1*Δ or WT overexpressing *MLG1* strains grown on synthetic defined media in the presence of 2% dextrose (SC) incubated with 1 nmol [^{14}C]palmitoyl-CoA (P-CoA) or [^{14}C]oleoyl-CoA (O-CoA). After incubation for 10 min, lipids were extracted and analysed by TLC and phosphorimaging as described in the Materials and methods. (A) The upper part shows the results in the presence of 1 nmol of commercial 1-18:1 lysoPS. The lower part shows the results in the presence of an extemporaneous preparation of 2-acyl lysoPS. (B) The results in the presence of 2-acyl lysoPE. A control without exogenous lysophospholipids (-) is included.

The results are representative of experiments performed with two independent homogenate preparations.

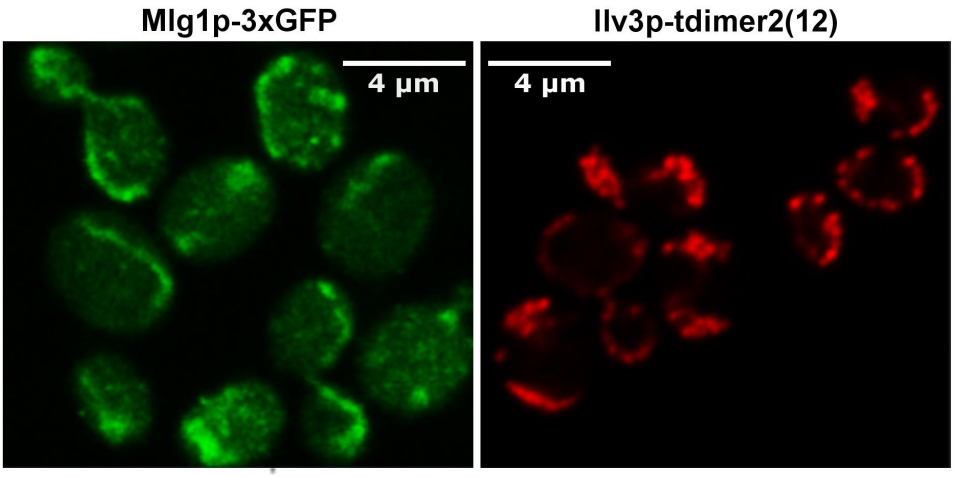

Fig. 8. Mlg1p is associated with a tubular network similar to the mitochondrial network in yeast cells. Labelled yeast cells with one single green fluorochrome (*i.e.* GFP) fused at the C-terminus of Mlg1p or with a red fluorochrome [tdimer2(12)] fused at the C-terminus of Ilv3 were used as control to ensure there was no bleed through between the green and red channels and to perform a preliminary analysis of the subcellular localisation of Mlg1p. BY4741 cells were grown in YPD media and harvested at the mid-logarithmic phase, then immediately analysed by confocal microscopy. GFP fluorescence was observed after excitation of the cells with a laser at 488 nm using the Airyscan super-resolution mode of the LSM880 microscope and the signal fluorescence emission observed from 526 to 606 nm.

Red fluorescence was observed from 588 to 642 nm following excitation with a laser at 561 nm.

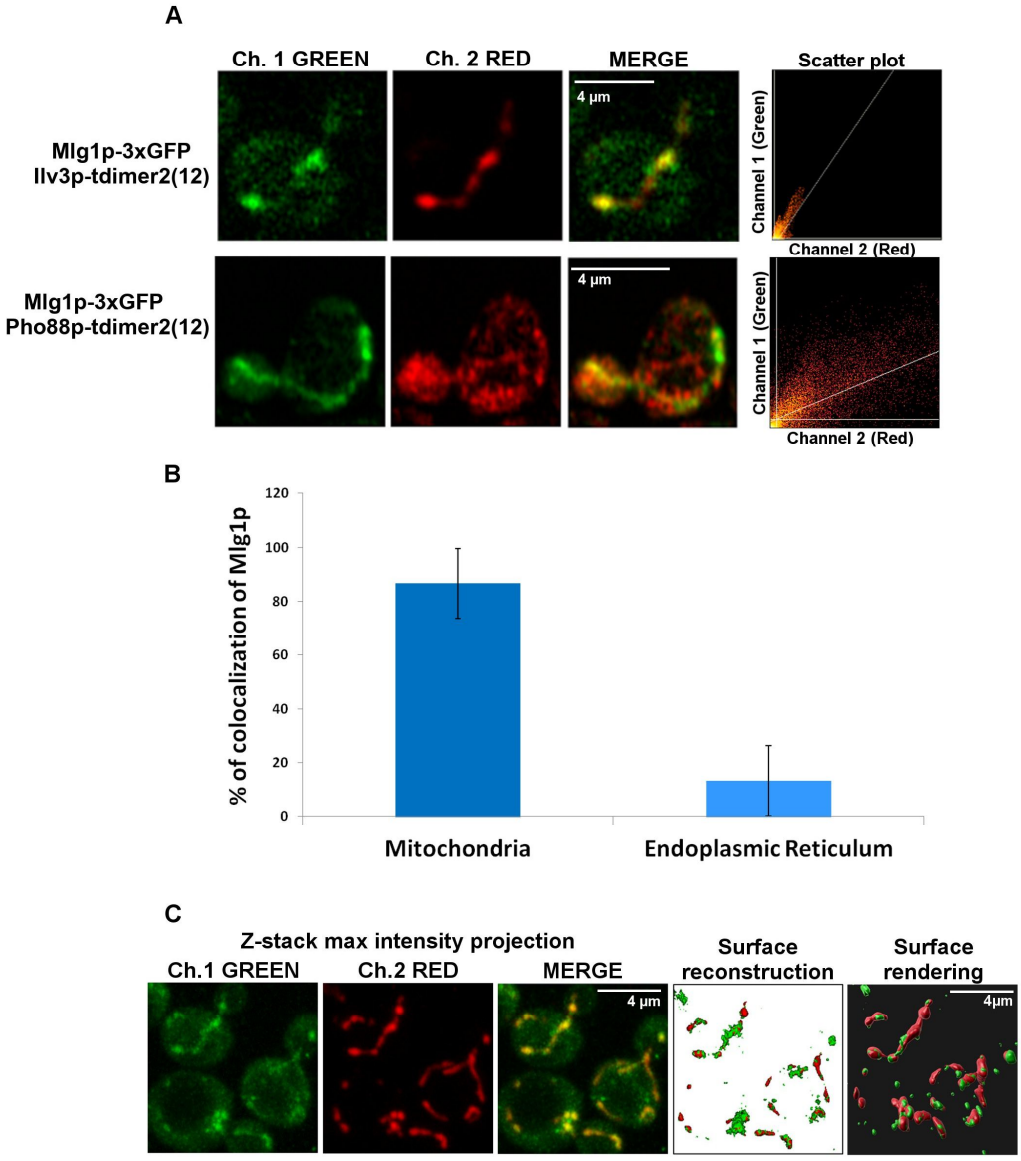

Fig. 9. Mlg1 is located in the mitochondrial area.

The subcellular localisation of Mlg1p was analysed by Airyscan confocal microscopy and compared with specific protein reporters like Ilv3p, which is associated with the mitochondrial compartment, and Pho88p, which is associated with the ER membranes. (A) Determination of subcellular localisation with BY4741 producing 3xGFP-tagged Mlg1p and either Ilv3p or Pho88p fused to tdimer2(12), a red fluorochrome. For each selected image, the scatterplots were generated using the FIJI co-localisation threshold plugin. They are shown at the right of panel A with channel 1 (GFP) pixel intensity along the x-axis and channel 2 [tdimer2(12)] pixel intensity along the y-axis with both the linear regression line as well as the thresholds marked. (B) The specific fluorescence merge signals were scored for each combination of the red and green fluorochromes, for at least three independent experiments in each case. The data are presented as the mean ± standard deviation, with n > 1000 cells for each combination (specifically, n = 1451 for Ilv3p and n = 1037 for Pho88p). (C) Z-stack maximum intensity projection from cells labelled with 3xGFP-tagged Mlg1p and Ilv3p fused to tdimer2(12) (left part of panel C) showed the maximum intensity projection for the green, red and merge channels. The Surface reconstruction panel is made by the 3D Zen black software. The surface rendering is made by the Imaris software.

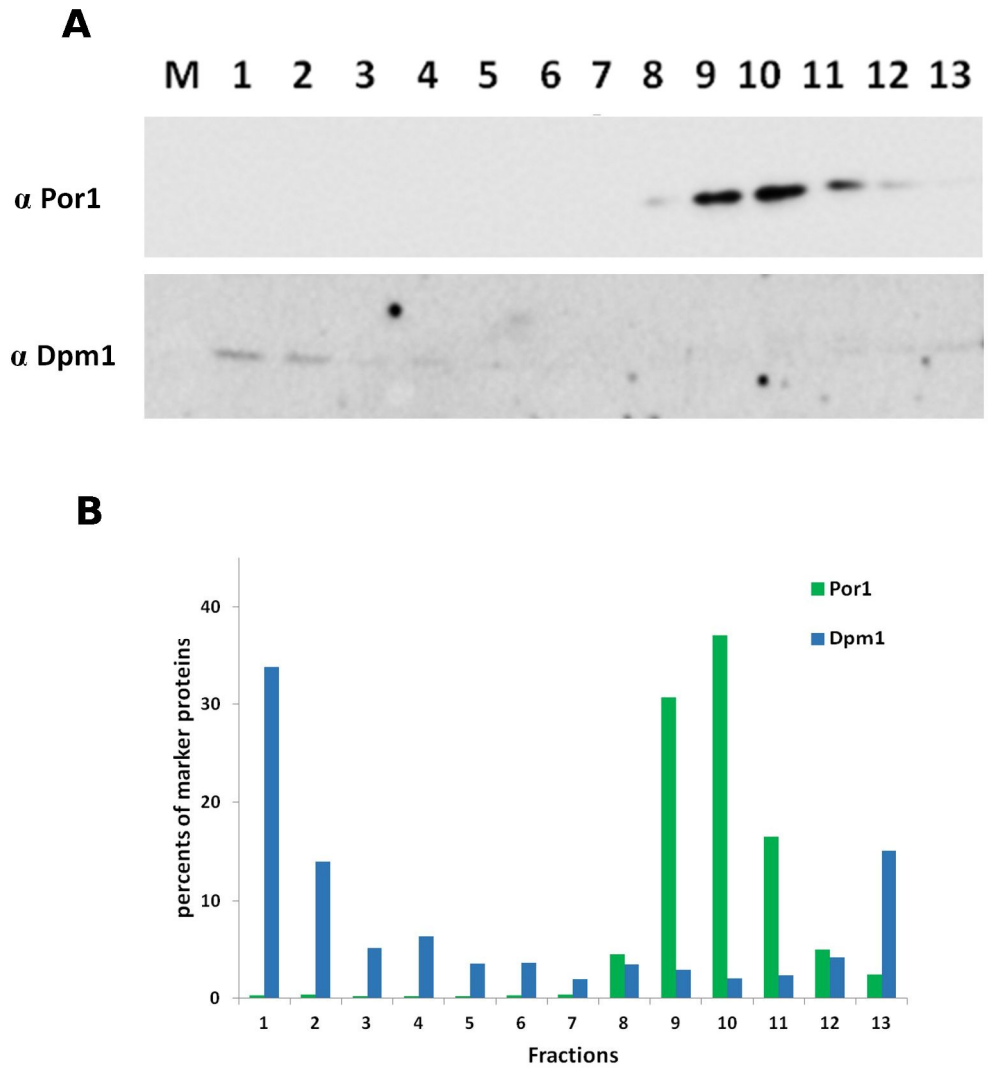

Fig. 10. Characterisation of mitochondrial fractions.

Crude mitochondria purified from BY4742 cells growing on SC-Gal medium were fractionated by ultracentrifugation at 100000 *g* for 16 h and at 4°C on 11 ml of a 20%–60% sucrose gradient with a preliminary centrifugation step at 30000 g for 1 h at 4°C. Fractions (750 µl) were collected from the top (F1) to the bottom (F14) of the gradient. (A) After electrophoresis on SDS-PAGE gels, proteins of each fraction were blotted on a nitrocellulose membrane for western blotting. Specific antibodies raised against the Porin (Por1, a specific mitochondrial outer membrane protein) and against Dpm1 (a specific marker of ER membranes) were used to identify the fractions containing mitochondria and Endoplasmic Reticulum. The

experiments were independently repeated four times. (B) Relative quantification of each fraction for the both protein markers specific for identification of mitochondria or ER membranes.

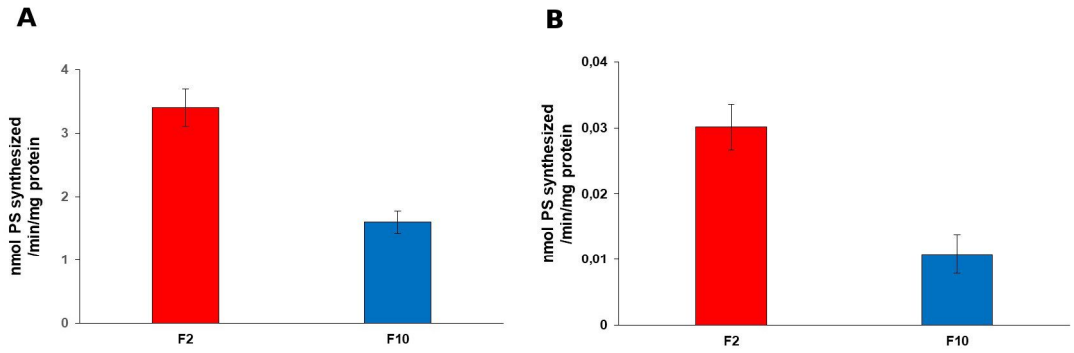

Fig. 11. LysoPS AT activities determined from highly purified mitochondria and MAMs purified from cells cultured on SC-Gal medium.

(A) Ale1p specific activity was determined using 0.5 nmol [^{14}C]oleoyl-CoA, 1 nmol of 1-18:1 lysoPS from a commercial preparation and 0.1 µg of protein from fractions 2 and 10. (B) Mlg1p specific activity was determined using 0.5 nmol [^{14}C]palmitoyl-CoA, 1 nmol of 2-acyl lysoPS from an extemporaneous preparation and 5 µg of protein from fractions 2 and 10. After incubation at 30°C, lipids were extracted and analysed as described in the Materials and methods. The results are presented as the mean ± standard deviation from one experiment (n = 4) and are representative of two distinct experiments.